# Dynamics of Thin Films Exposed to Vibrations

Marina Markaki & Denisse Mendoza

Department of Mathematics, New Jersey Institute of Technology

MATH451H

Professor Lou Kondic

May 11, 2022

**Table of Contents**

# Introduction

## Motivation and Original Approach

Acoustics are known to influence fluid motion. Recent experiments were performed in which acoustic driving was used to produce targeted motion of different fluids. This experimental setup involved fluids spreading on substrates. Oil film responds to acoustic driving, while water drops don't. So in theory, acoustic driving could be used to separate oil and water. The problem of solving coupled partial differential equations (PDEs) is being reduced by considering modeling coupling between fluid motion and acoustics in terms of simplified models.

The original motivation for this project involved simulating a fluid coating another one with a driving force. We approached this simulation by expanding on an easy original problem. We started with a discretized model of a fluid droplet on an angled plane with gravity being the driving force. In an attempt to simulate coating of a fluid, we then added an obstacle to our model. Eventually, we moved to modeling the spreading of a single droplet, by considering a flat plane. Finally, we introduced vertical vibrations on a flat surface and the closing of a hole with said vibrations.

## Fluid Dynamics with Vertical Vibration

Vibrations of a substrate could strongly influence dynamics of evolving thin films. In our project we consider thin liquid films on a horizontal, solid, and completely wetting substrate. The substrate is subjected to oscillatory accelerations in the normal direction. A linear Floquet analysis shows that the planar film surface loses stability if amplitudes and frequencies of the harmonic oscillations meet certain criteria. Normal oscillations show the traditional Faraday

patterns, such as squares and hexagons, while lateral oscillations cause a pattern formation scenario similar to spinodal dewetting (the process of retraction of a fluid from a non-wettable surface it was forced to cover [4]). A combination of normal and lateral oscillations, with specific amplitude and frequency ranges, can allow a droplet to travel in a horizontal plane.

The present project focuses on the results of recent experiments showing that vertical oscillations may influence closing of a dry spot existing in a thin film. We used existing models for thin films and included vibrations by imposing time-dependent sinusoidal gravity and implementing the experimental parameters. We confirmed spatial and temporal convergence of the implemented computational routine and explored the influence of vibration parameters, namely amplitude and frequency, on how fast a hole closes.

Physicist, Michael Bestehorn, argues for the existence of $d_c$, a critical diameter for holes in a liquid [2]. If the hole, for a given volume of fluid in a container of a given size, has a diameter greater than $d_c$, then the hole is considered stable and will not close with gravity alone. On the contrary, if the diameter is greater than $d_c$, the hole is unstable and will close. Our project does not take $d_c$ into consideration. In fact, our hole models are performed with unstable holes that will close regardless. We are interested in how vibrations affect the time the holes will take to close.

## Derivation of the Equation

In this project, we want to derive the non-dimensional thin film equation with vibration, in order to get the correct values for the amplitude and frequency. Firstly, we start with the Navier Stokes equation with vibration shown below:

$$\frac{\partial \bar{u}}{\partial \bar{t}} + (\bar{u} \cdot \bar{\nabla})\,\bar{U} = -\frac{1}{\rho}\,\bar{\nabla}\,\bar{\rho} + \frac{\mu}{\rho}\,\bar{\nabla}^2\,\bar{u} - g(1 + e\,sin(\bar{\omega t})) \quad (1)$$

Then, after some boundary and initial conditions, that we will not be covering, we end up with

$$\frac{dh}{dt} = -\frac{1}{3\mu}\nabla\left(\gamma \bar{h}^3 \nabla^3 \bar{h} - \rho g(1 + a(t))\bar{h}^3 \nabla \bar{h} + \rho g \bar{h}^3 b(t)\,\hat{i}\right) \quad (2)$$

which is the dimensional thin film equation. a(t) and b(t) correspond to normal and lateral accelerations respectively, both measured in units of g. In order to nondimensionalize it, we substitute $x = \frac{\bar{x}}{x_c}$, $h = \frac{\bar{h}}{h_c}$, $t = \frac{\bar{t}}{t_c}$ and distributing the negative sign, we end up with

$$\frac{h_c}{t_c}\frac{dh}{dt} = \frac{1}{3\mu}\frac{1}{x_c}\nabla\left(\rho g(1 + a(t))h^3 h_c^3 \nabla h\,\frac{h_c}{x_c} - \gamma h^3 h_c^3 \nabla^3\, h\frac{h_c}{x_c^3} - \rho g h^3 h_c^3 b(t)\,\hat{i}\right) \quad (3)$$

After combining like terms, we end up with this:

$$\frac{h_c}{t_c}\frac{dh}{dt} = \frac{1}{3\mu}\frac{1}{x_c}\nabla\left(\rho g(1 + a(t))h^3 \nabla h\,\frac{h_c^4}{x_c} - \gamma h^3 \nabla^3\, h\frac{h_c^4}{x_c^3} - \rho g h^3 h_c^3 b(t)\,\hat{i}\right) \quad (4)$$

After dividing both parts with $\frac{h_c}{t_c}$ and factor out the coefficient on the $h^3\nabla^3$ term to get:

$$\frac{dh}{dt} = \frac{\gamma t_c h_c^3}{3\mu x_c^4}\nabla\left(\frac{x_c^2 \rho g}{\gamma}(1 + a(t))h^3 \nabla h - h^3 \nabla^3 h - \frac{x_c^3 \rho g}{h_c \gamma} h^3 b(t)\,\hat{i}\right) \quad (5)$$

Now we can choose $x_c$ so that our last coefficient equals to 1: $\frac{x_c^3 \rho g}{h_c \gamma} = 1 \Leftrightarrow x_c = \left(\frac{h_c \gamma}{\rho g}\right)^{1/3}$:

$$\frac{dh}{dt} = \frac{\gamma t_c h_c^3}{3\mu x_c^4}\nabla\left(\frac{x_c^2 \rho g}{\gamma}(1 + a(t))h^3 \nabla h - h^3 \nabla^3 h - h^3 b(t)\,\hat{i}\right) \quad (6)$$

Now we can choose $t_c$ so that our outer coefficient equals to 1: $\frac{\gamma t_c h_c^3}{3\mu x_c^4} = 1 \Leftrightarrow t_c = \frac{3\mu x_c^4}{\gamma h_c^3}$:

$$\frac{dh}{dt} = \nabla\left(\frac{x_c^2 \rho g}{\gamma}(1 + a(t))h^3 \nabla h - h^3 \nabla^3 h - h^3 b(t)\,\hat{i}\right) \quad (7)$$

We let $D = \frac{x_c^2 \rho g}{\gamma}$ , a(t) equals the amplitude-frequency equation we use in our code [εsin(ωt)] and since in our case we are only considering vertical accelerations, we can set b(t) equal to 0 and remove it from the equation:

$$\frac{dh}{dt} = \nabla\left(D(1 + \varepsilon sin(\omega t t_C))h^3 \nabla h - h^3 \nabla^3 h\right) \quad (8)$$

Finally we distribute the ∇ to get the final non-dimensional thin film equation with vibration:

$$\frac{dh}{dt} = D(1 + \varepsilon sin(\omega t t_C))\nabla[h^3 \nabla h] - \nabla[h^3 \nabla^3 h] \quad (9)$$

For our numerical solution we use the capillary length of water $l_c = \sqrt{\frac{\gamma}{\rho g}}$ and the thickness of an infinite unbounded liquid layer $h_c = 2 \cdot l_c$ .

| **Parameter Values** | | |
|---|---|---|
| **Symbol** | **Physical Meaning** | **Quantitative Value** |
| ρ | Density of Water | $10^3 [\frac{kg}{m^3}]$ |
| γ | Surface Tension of Water | $0.07275\ [\frac{kg}{s^2}]$ |
| μ | Dynamic Viscosity of Water | $8.9 \cdot 10^{-4} [\frac{kg}{m \cdot s}]$ |
| g | Gravity | $9.8 [\frac{m}{s^2}]$ |
| $l_c$ | Capillary length | $0.00272\ [m]$ |

| | | |
|---|---|---|
| $h_c$ | Characteristic Film Thickness | $0.00544\ [m]$ |
| $t_c$ | Characteristic Time Scale | $3.1496 \cdot 10^{-5}[s]$ |
| $x_c$ | Characteristic Length Scale | $0.00343\ [m]$ |

For our ε and ω we used typical values observed in the experiment. The vibration amplitude was usually fixed to values ranging between 0 and 75 $\frac{m}{s^2}$. For the frequency, 170 Hz was mostly used, otherwise 65 or 100 Hz was used.

**Discretization**

In order to model the thin film numerically, we had to discretize the equation. The $\nabla[h^3\nabla^3 h]$ term gives us a 4th derivative, which could require 4 ghost points on one side if not chosen wisely. Our code which was inherited from the code used to model a fluid on a funnel, used the equation in the following form:

$$\frac{dh}{dt} = -\ \nabla\{h^3[\nabla(\nabla^2 h)\ -\ D(1\ +\ \varepsilon sin(\omega t t_C))\nabla h]\}$$

The inner derivative in the $\nabla(\nabla^2 h)$ term uses central difference while the outer derivative uses backward difference. When discretized, it's essentially represented as $\nabla(\nabla^2 h(x_i)) = \frac{-f(x_{i-2})+3f(x_{i-1})-3f(x_i)+f(x_{i+1})}{dx^3}$. The derivative in the $D(1\ +\ \varepsilon sin(\omega t t_C))\nabla h$ term simply uses backward difference with the final outer derivative of the entire expression using forward difference. Discretizing in this way allows us only to require 4 ghost points, 2 on either side of the length of the surface.

A boundary we imposed are making $h_{xxx} = 0$ at the bounds. This was to ensure that the boundary remained constant.

## Models and Simulations

We began programming with an existing set of code that simulated fluid traveling down a funnel. The code contained the numerical solution of the PDE, discretized using polar coordinates. We converted the model into cartesian coordinates and tweaked the equation to remove the elements that related to a funnel, and changed them to represent fluid on an inclined plane. With this code we were able to produce several different models by altering only specific lines of code.

### Fluid on an Inclined Plane

As mentioned, our first task consisted of changing the code from polar to cartesian. We also had to change the model as the code was written for fluid traveling down a funnel which changed some parts of our thin film equation. In particular, we needed to remove a part of the code that accounted for the substrate curvature, $\frac{tan(\theta)}{r}$. As a result, our model simulated a cross section view of a fluid droplet traveling down an inclined plane. Our model shows only a cross-section view of the droplet as in the figure below. We only consider the x and z axes in our model as we only account for the direction in which the fluid travels, caused by gravity, and the height of the fluid throughout its trajectory. In our model, however, the highest point of the incline is actually on the right side, with the fluid traveling towards the left.

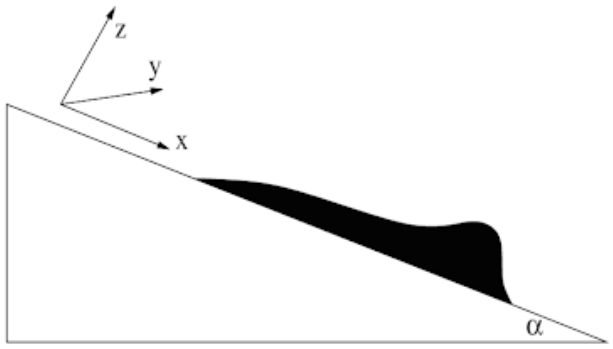


We used $\alpha = \frac{47\pi}{180}$ and ran the simulation and got the results shown below. It shows how the height of the fluid changes as time goes by.

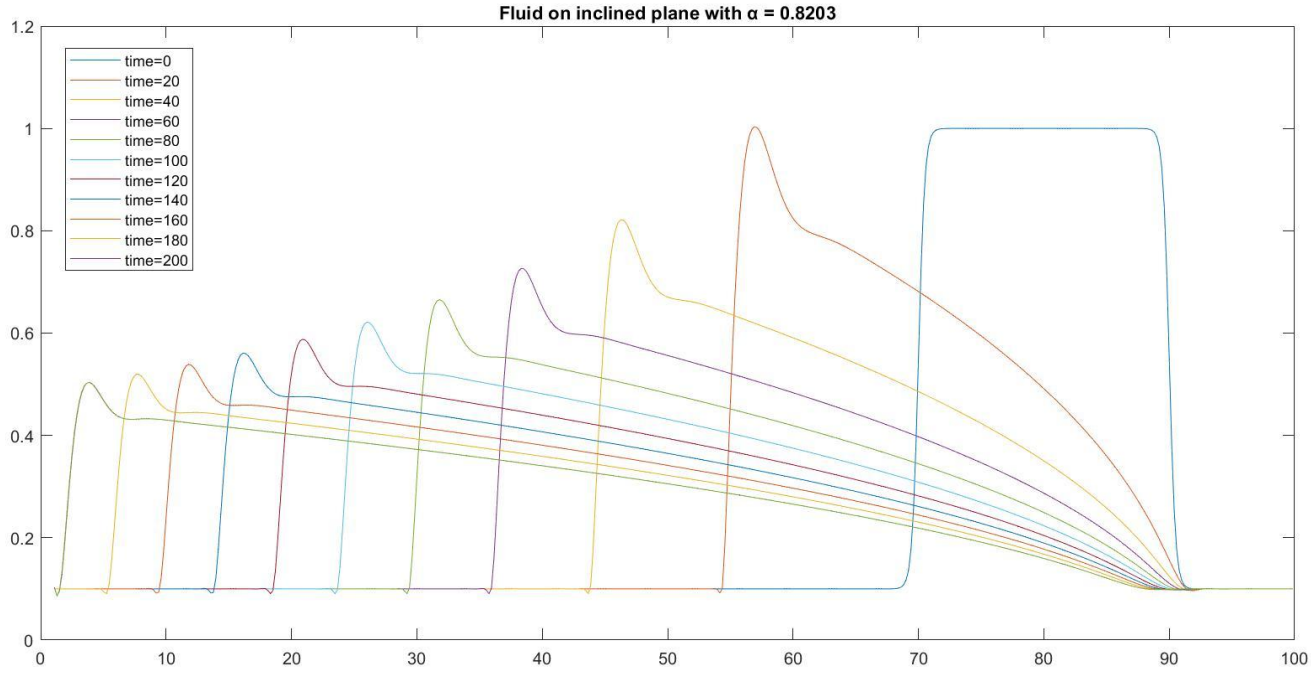


**Fluid with an Obstacle**

Since our original goal involved using vibrations to "coat" one fluid with another, we took the direction of introducing an obstacle into our simulation. We kept the same angle as in the previous simulation but in this case, added a substrate with the fluid lying above it. In graphs

(a) through (f), the flow of the liquid is represented by the orange plot, while the obstacle is depicted with the blue plot. The liquid here also flows from right to left. As seen by the plots, with time, the fluid does eventually go over the obstacle and leave behind a “residue” both over the substrate and obstacle.

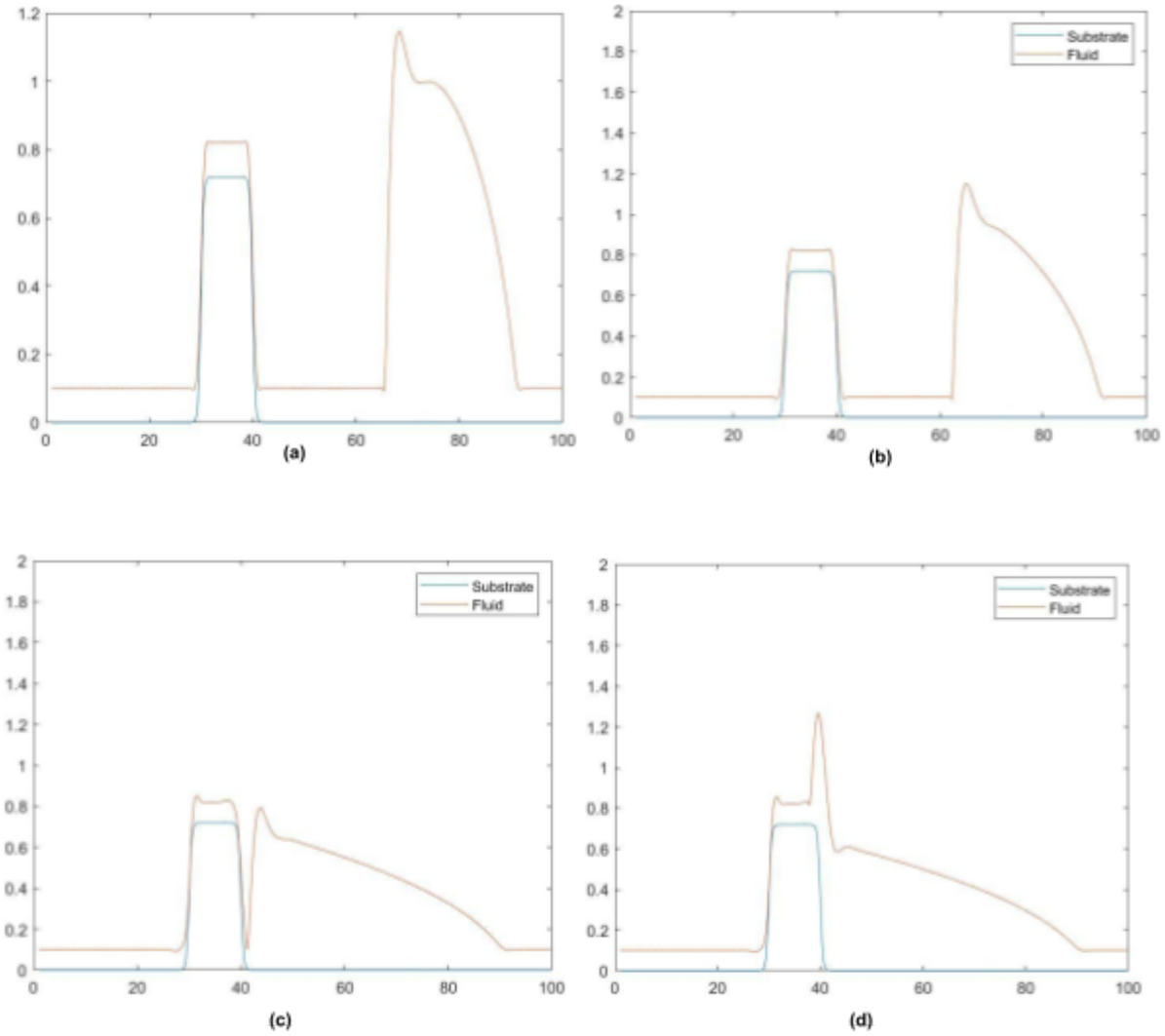

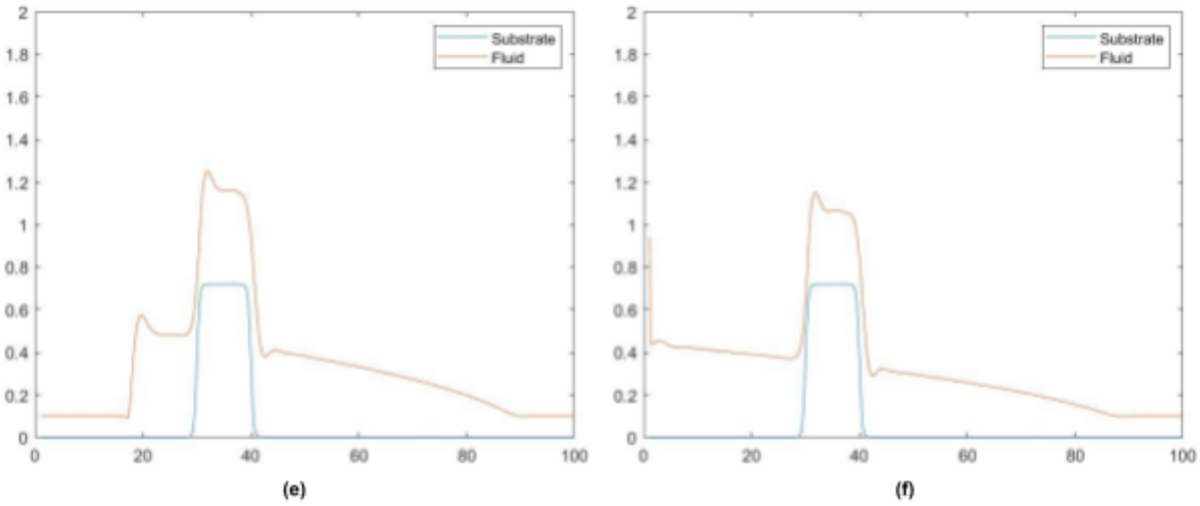


**Fluid Spreading on a Flat Surface**

As a next step to simulate one liquid coating another one, we wanted to ensure that our model still adhered to the characteristics of fluid dynamics on a thin film when on a flat plane. To simulate this, we made α = 0 while keeping gravity constant as in the previous simulations. We made our initial condition a fluid with a height of $0.75\ t_c$ and a width of $40\ x_c$ at the center of our $100\ x_c$ surface. We expected the fluid droplet to flatten as time progressed. We also anticipated the fluid to equally distribute on both sides. The motion of the fluid is shown below in graphs (a) through (e). As shown in the figures, the liquid did in fact "flatten" out equally on both sides. Also, it's important to note that the liquid achieved this after a very long period of time. The motion of the fluid was much slower in this case than for $\alpha > 0$.

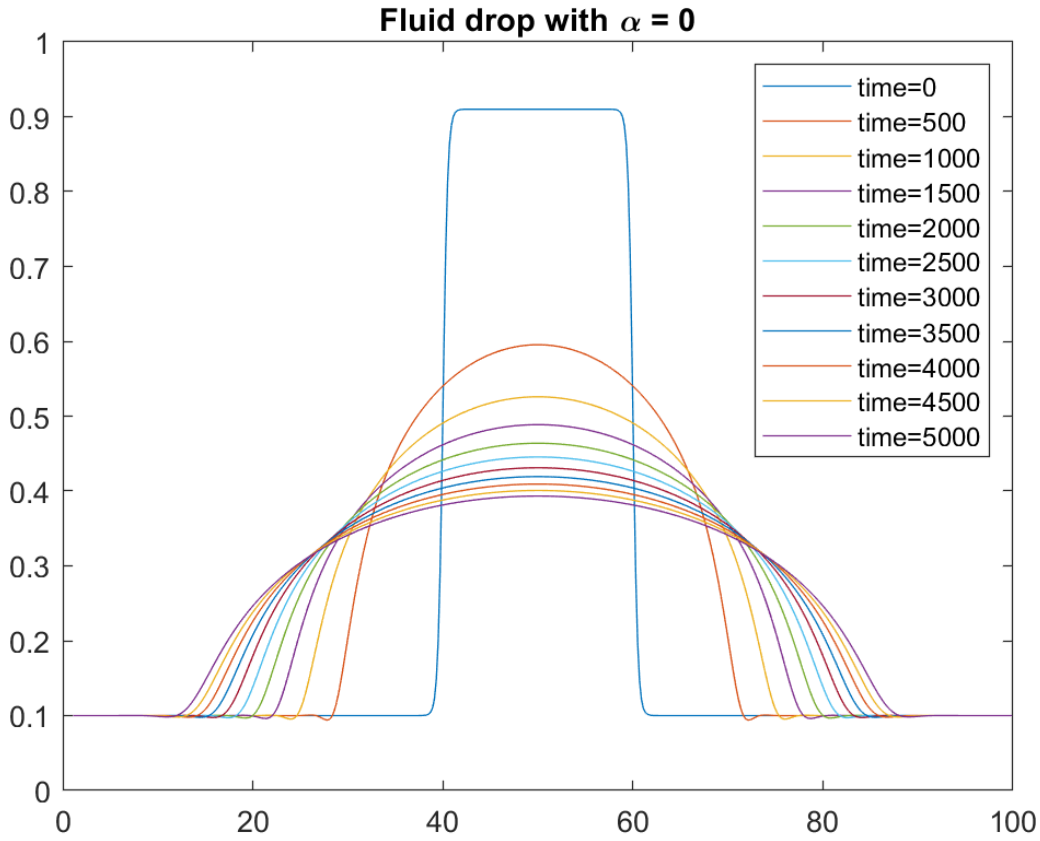


So as the figures above show, the model did reflect what we expected for a fluid on a flat plane. We wanted to ensure that our model was meeting certain checks and criteria. Specifically, we wanted to check that the fluid's volume remained constant while time elapsed. Below is a figure that shows the area under the curve on the figure with different choices of $dx$.

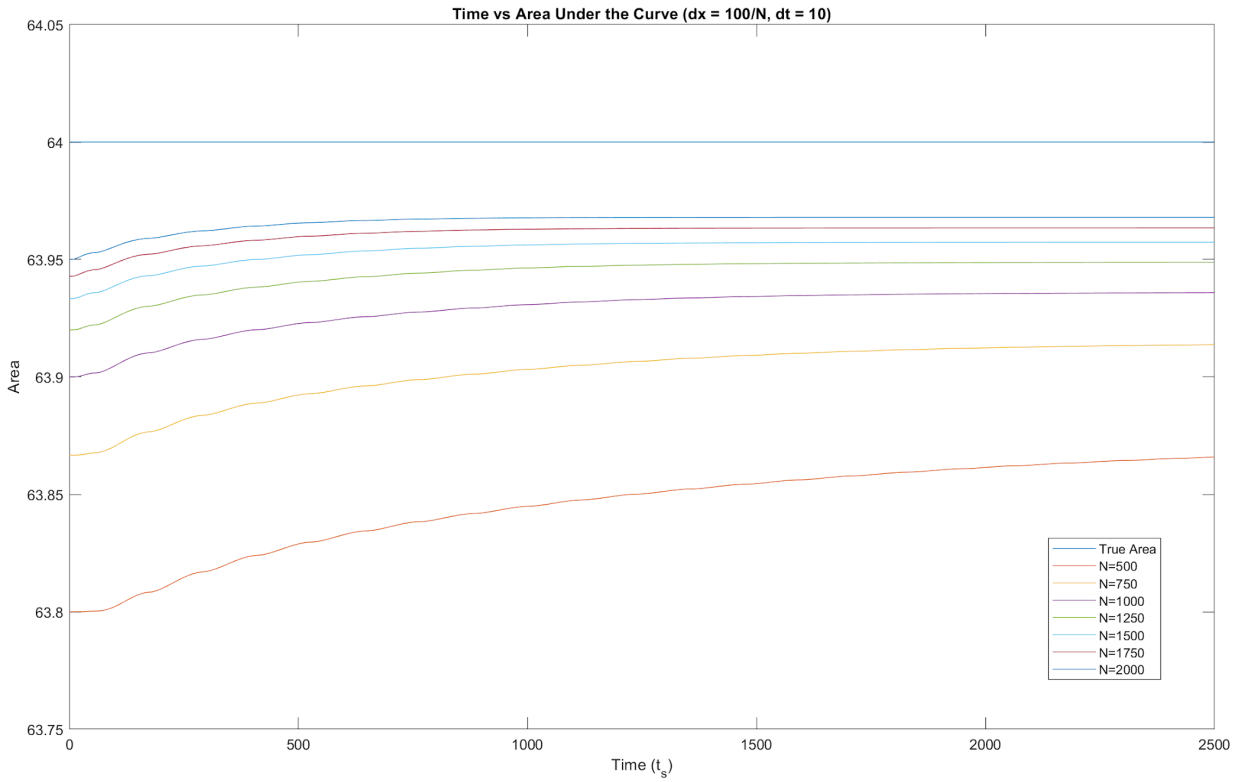


As seen in the figure, the smaller our $dx$, the more precise the area under the curve. Also, something interesting, is that for each value of $dx$, the curve rose to some asymptote which is also closer to the true area under the curve. We used the trapezoid rule to evaluate these areas and believe that this method and the shape of the fluid droplet as it spreads may contribute to this. As the droplet flattens out, the area of each individual trapezoid will be more and more precise, which explains the asymptotic behavior. Similarly, a smaller $dx$ leads to a smaller error.

**Introducing Vibrations: Flat Vibration**

Once our models showed promising and consistent results, we shifted gears and directed our research towards vibrations. For our previous models, the only force acting on the fluid droplet was gravity, which remains constant throughout the process. If we can cause a sinusoidal

fluctuation in gravity with respect to time, this can represent vibration. We let this fluctuation in gravity be represented by the equation $1 + \varepsilon sin(\omega t)$ where $\epsilon$ represents the vibration amplitude and $\omega$ represents the angular frequency. This expression is multiplied by $g$ in our equation to have the magnitude of acceleration oscillating.

The images below show an initial condition of 10 waves. These 10 waves are put under a vibrating force. As shown in the 4 figures below, the waves still flatten out as we saw with the fluid spreading on a flat surface in the previous model. However, the liquid does appear to be vibrating with the amplitude expanding slightly and then further decreasing.

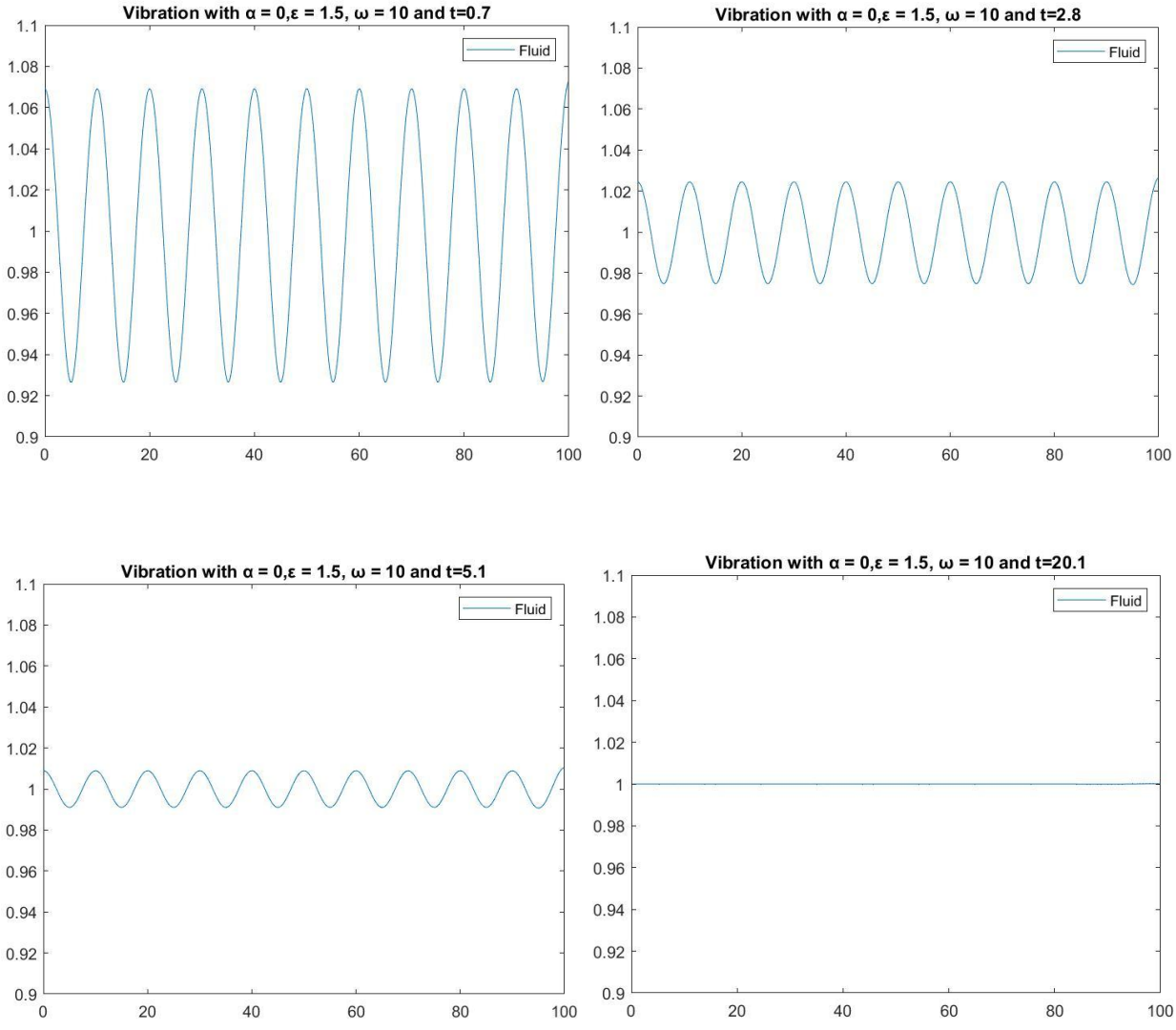

Since the vibrations can not be depicted through the graphs above, we generated a plot of the maximum height of the vibration through time using two different values of ε. As shown, when gravity is constant (ε = 0), the fluid converges to one height smoothly. However, when introducing vibration (ε = 1.5), there is a fluctuation in the heights of the fluid.

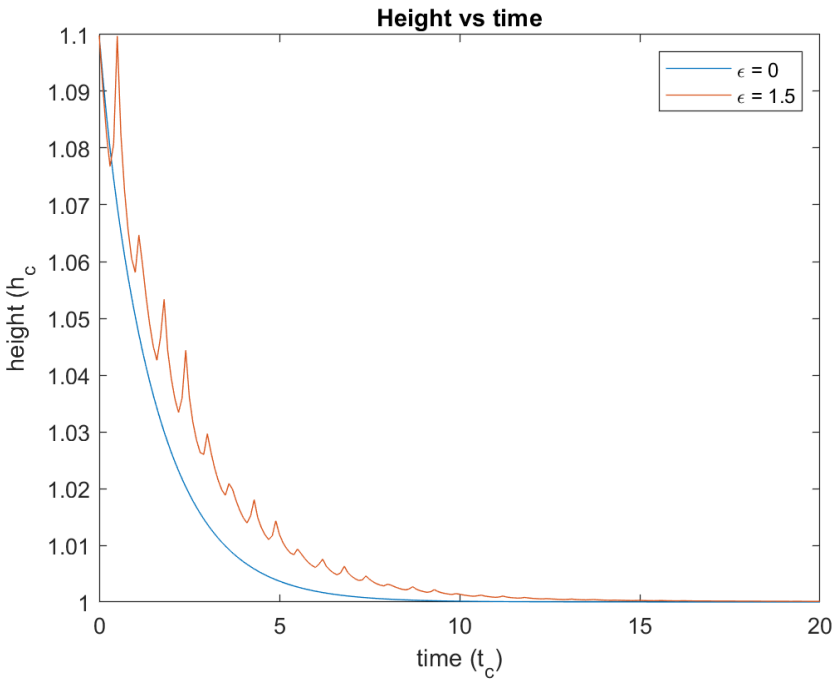


**Incorporate holes (Cup)**

Finally, we began exploring the effects of vibrations on the closing of holes. We had to determine how we wanted to mathematically represent the closing of the holes. We decided to track two measures: the time both sides of the fluids take to "touch" and the time they take to "fully close". Since our initial condition had the hole centered around $x = 50$, we defined the time to touch as the time it takes for the minimum height to be found at the center. We define the time to close as the time it takes for the maximum and minimum height to have an absolute difference of some tolerance. We chose a tolerance of 0.05.

We consider an initial condition of a film that reaches a height of $1\,h_c$ with a film thickness of $0.1\,h_c$. The film expands the $100\,x_c$ length. There is a hole centered at $x = 50x_c$ with a width of $40\,x_c$. We want to compare how long the hole takes to close for constant gravity compared to when vibration is introduced. To simulate constant gravity, we simply made ε = 0 and found that the times to touch and times to close were 628.9 and 1646.7 $t_c$ respectively. However, interesting things happened when we varied the values of ε. Below is a table showing the different times for changing values of ε.

**Different ε when using ω = 170**

| **ε** | **Time to touch** | **Time to close** |
|---|---|---|
| 0 | 628.9 | 1646.7 |
| 1 | 608.6 | 1586 |
| 2 | 521 | 1553 |
| 3 | 455.3 | 1208.2 |
| 4 | 780.3 | 1384.8 |

**Different ω when using ε =3**

| **ω** | $\overline{\omega} = \omega t_c$ | **Time to touch** | **Time to close** |
|---|---|---|---|

| | | | |
|---|---|---|---|
| $2\pi \cdot 65$ | $\approx 0.012863$ | 209.9 | 1635 |
| $2\pi \cdot 80$ | $\approx 0.015831$ | 402.4 | 1733.6 |
| $2\pi \cdot 95$ | $\approx 0.018800$ | 420.9 | 1766.4 |
| $2\pi \cdot 110$ | $\approx 0.021768$ | 404.1 | 1793.3 |
| $2\pi \cdot 125$ | $\approx 0.024736$ | 396.7 | 1637.5 |
| $2\pi \cdot 140$ | $\approx 0.027705$ | 464.7 | 1649.8 |
| $2\pi \cdot 155$ | $\approx 0.030673$ | 479.3 | 1662.6 |
| $2\pi \cdot 170$ | $\approx 0.033642$ | 455.3 | 1208.2 |

We chose the different values of ε and ω, based on scaling. Knowing that angular frequency gives $\omega = 2\pi f$ and since it does have a dependency on time, we scaled it down with respect to $t_C$. That made $\overline{\omega} = \omega \cdot t_C = 2\pi(f)t_C$ , where f came from the experimental results mentioned in page 7. For $f$, we chose values 65-170, since these were the values used in the experiment. Since gravity is being multiplied to our amplitude-frequency equation $(1 + \varepsilon sin(\omega t))$, amplitude is being scaled down only by g, so $\varepsilon = \frac{a}{g}$, where $a$, our amplitude, came from the experimental results mentioned in page 7. While we had originally planned to use values 0-8 to match the experimental parameters, we had some significant numerical errors the higher ε was, limiting our valuable results for $0 \leq \varepsilon \leq 4$. Below there is a visual representation of how time changes when the values of amplitude and frequency increase.

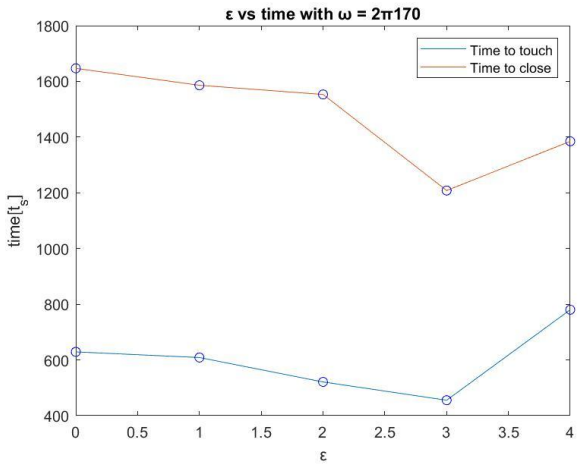


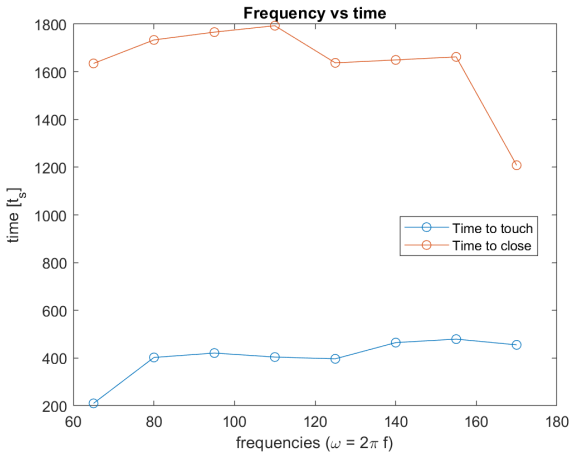


## Conclusion

It's important to note that for high values of epsilon, we had significant numerical problems, namely, the vibrations were showing very high amplitudes, much higher than the maximum height of our initial condition of the hole. Secondly, we realized that we could have better defined how to represent the touching and closing of a hole. We observed that for certain values of ε and ω, the hole appeared to almost close before being "interrupted" by a vibration that increased the amplitudes again. To find a way around this, we could have either increased our tolerance, or redefined our criteria to use a standard deviation as opposed to the difference between the maximum and minimum values.

With that said, our models show a slight relationship between characteristics of a vertically vibrating force and the time a liquid takes to drop and spread. In the ε vs time figure, it can be seen that a higher amplitude does decrease the time it takes for a hole to close and merge. This doesn't hold true for $\varepsilon = 4$ because at this point, our model started becoming sensitive to the high-amplitude waves. Moreover, the ω vs time figure doesn't show a very clear relationship

between the frequency and time to close. We believe this may be due to the way we defined closing and merging, as described earlier.

This relationship can be useful in experiments regarding our original motivation, using acoustics to lead a fluid droplet to cover and coat another. The frequency and amplitude of the vertical vibrations can be used to control the spreading. Furthermore, we know that a hole will only close if it's unstable. Perhaps, the introduction of vertical vibrations can influence the closing of holes that otherwise wouldn't.

We faced some challenges throughout the duration of our research. In the beginning of our project, we decided to use the code that was used for Dijksman and Kondic's thin film in a funnel, with the goal of changing it to match our models. While we believed that using existing code would be easier, it was challenging trying to understand their code, which used polar coordinates and had some elements of a funnel, and change it to cartesian coordinates with only the parts of the thin film equation that we were concerned with. Moreover, once we got our code to work properly, it took some time for our project to take a true direction and ultimately we focused on vibrations, albeit somewhat towards the end of our semester.

There is a lot of room for growth here, as we only ever got to analyze the effects of vibration on closing holes that were already unstable. There are models that can be made with stable holes as the initial condition. There can also be an obstacle introduced to the model to see how the vibrations affect spreading in that case. There is also a lot that can be discovered with the introduction of lateral vibrations, which we did not include in our research.

## Matlab Code

Below is the main function we used to solve the PDE. The MATLAB code for each simulation is submitted separately along the report.

```
function F = myfun(~,h)
    %% Ghost points outside the computational domain
    % hn1 = h(R-dr/2)
    % hn2 = h(R-3*dr/2)
    % hp1 = h(L+dr/2)
    % hp2 = h(L+3*dr/2)
    % NOTE!!
    % The boundary conditions related to hn2 and hp2 are imposed later,
    % so these two points need not to be defined here,
    % we simply assign 0 to them.
    sh=h+sub;
    shl1 = sh(1);
    shl2 = sh(2);
    shr1 = sh(N);
    shr2 = sh(N-1);
    hn1 = h(1);
    hp1 = h(N);
    %% h3: Evaluate h^3 at N+1 regular grid points
    h3 = ([h.^3;hp1^3]+[hn1^3;h.^3])/2;
    %% tmp1: Evaluate h_x_x at N+2 grid points (central difference)
    % tmp1 = ([h;hp1;hp2] - 2*[hn1;h;hp1] + [hn2;hn1;h])/(dr^2);  %central
    FDpos=([sh;shr1;shr2]-[shl1;sh;shr1])/dx; %backward difference (1 to 502)
    FDneg=([shl1;sh;shr1]-[shl2;shl1;sh])/dx; %backward difference (0 to 501)
    tmp1=(FDpos-FDneg)/dx; %forward difference (0 to 501) (same as central)
    %%tmp2:Evaluate ((1/r)(r*h_r)_r)_r -TA/r^2 - G*(SA+CA*h_r) at N+1 points
    % NOTE!!
    % Some boundary conditions are imposed here
    % Evaluate h_x_x_x at N+1 grid points (backward difference 1-501)
    tmp2 = (tmp1(2:(N+2)) - tmp1(1:(N+1)))/dx;
    % Boundary condition: h_x_x_x=0 at r=R=L
    tmp2(1)=0;
    tmp2(N)=0;
    % Evaluate h_x_x_x - D*h_x at N+1 grid points
    h_x=FDpos(1:N+1);
    %tmp2 = tmp2 - G*D*CA*([sh;shr1]-[shl1;sh])/dx;
    tmp2 = tmp2 - V*(h_x); %3rd derivative
    % Boundary condition: ((1/r)(r*h_r)_r)_r - G*CA*h_r=0 at r=L
    % Evaluate h_x_x_x - D*h_x - 1 at N+1 grid points
    tmp2 = tmp2 - SA;
    %% Q: Evaluate h3*(h_x_x_x - D*h_x - 1) at N+1 grid points
    Q = h3.*tmp2; %flux
    %% F = Q_x (forward difference)
    F = -(Q(2:N+1)-Q(1:N))./(dx);
end
```

## Citation

[1] Michael Bestehorn , "Laterally extended thin liquid films with inertia under external vibrations", Physics of Fluids 25, 114106 (2013) https://doi.org/10.1063/1.4830255

[2] Cunjing Lv, Michael Eigenbrod, Steffen Hardt, “Stability and collapse of holes in liquid layers”, J. Fluid Mech, 1130–1155 (2018)

[3] T.-S. Lin, J.A. Dijksman, Lou Kondic, “Thin liquid films in a funnel”, J. Fluid Mech. (2021)

[4] Wikimedia Foundation. (2021, December 2). Dewetting. Wikipedia. Retrieved April 22, 2022, from https://en.wikipedia.org/wiki/Dewetting